



Fabrication of nano-platinum alloy electrocatalysts and their performance in a micro-direct methanol fuel cell

Mehdi Mehrpooya^{1,a}, Farzad Valizadeh¹, Reza Askarimoghadam¹, Sadegh Sadeghi², Fathollah Pourfayaz¹, Seyed Ali Mousavi¹

¹ Department of Renewable Energies and Environment, Faculty of New Sciences and Technologies, University of Tehran, Tehran, Iran

² Department of Chemistry, Faculty of Science, Tarbiat Modares University, Tehran, Iran

Received: 5 March 2020 / Accepted: 13 July 2020 / Published online: 22 July 2020

© Società Italiana di Fisica and Springer-Verlag GmbH Germany, part of Springer Nature 2020, corrected publication 2020

Abstract The main target of this investigation is to propose an effective anodic electrocatalyst for micro-direct methanol fuel cell. For this purpose, five nanostructured metal alloy electrocatalysts including platinum (Pt), ruthenium (Ru) and iron (Fe) are synthesized. The single-walled and multi-walled carbon nanotubes (SW-CNT and MW-CNT) and graphene (Gr) are employed as the carbon (C) base. First, PtRuFe/SW-CNT, PtRuFe/MW-CNT, PtRuFe/Gr and PtRuFe/C catalysts with a 1:4:5 atomic ratio for Pt, Ru and Fe, respectively, and PtRu/C catalyst with a 1:1 atomic ratio for Pt and Ru, correspondingly, are prepared by the process of improved alcohol recovery. In continuation, the morphology and activity of synthesized nano-electrocatalysts are confirmed and assessed by applying the physical and electrochemical tests. According to the obtained results, PtRuFe/SW-CNT is the most suitable catalyst for methanol oxidation reaction. The outcomes of electrochemical measurements show that PtRuFe/SW-CNT electrocatalyst has the highest activity, mass activity, mass transfer and electrochemical active surface area with respect to methanol oxidation in comparison with the commercial Pt/C and the rest of the synthesized catalysts. Next, two-electrode membrane assembly is fabricated with PtRuFe/SW-CNT and commercial Pt/C electrocatalysts to evaluate the performance of them in micro-direct methanol fuel cell. Based on the obtained polarization curves, by using PtRuFe/SW-CNT instead of commercial Pt/C, the current density in zero-voltage and maximum power density enhance by 48% and 92.3%, respectively.

1 Introduction

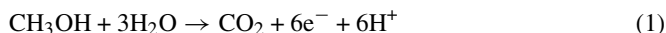
Because of increasing population of world and energy consumption, fossil fuels cannot be a sustainable and suitable resource for providing the required energy [1]. Also, due to the high amounts of CO₂ and NO_x emissions by applying fossil fuel power plants, they are very harmful for human health and environment [2]. Utilization of the green resources can be a

The original version of this article was revised: The authors regret that the first name of Fathollah Pourfayaz was spelled incorrectly in the author list.

^a e-mail: mmhrpuya@gmail.com (corresponding author)

proper and promising solution in order to overcome environmental concerns. Fuel cells are one of the zero pollution and efficient technologies. Fuel cell is a converter component that converts the chemical energy of fuel into direct electricity by electrochemical reactions [3]. Fuel cells have several important applications such as portable computers, aircrafts, power plants, hospital and buses [4]. Among the conventional power generation plants, fuel cells have a high electrical efficiency, but due to the some economical and technical problems, this technology needs a higher development for commercial applications [5]. Direct methanol fuel cell (DMFC) due to their benefits such as easy transport, independent of system size, high reliability, utilizing liquid fuel, high efficiency and high specific energy of methanol (6 Wh/g), can be employed as small portable power source [6, 7]. The performance and efficiency of the fuel cells depend largely on the type of catalysts, which are employed at the anode and cathode sides. Platinum (Pt) is the most common catalyst, which is utilized for oxygen reduction reaction (ORR) at cathode side, and methanol oxidation reaction (MOR) at anode side [8]. The electrochemical reactions occurred at the anode and cathode sides of the DMFC can be written as follows [9]:

Anode side (MOR):



Cathode side (ORR):



Overall reaction:



Although Pt is a suitable and efficient catalyst for DMFC, some problems such as limited availability, high cost, CO adsorption on Pt surface, and low utilization efficiency, the utilization of them have been limited [10]. Pt alloying with other metals is a proper method in order to rectify the MOR and ORR activity [11]. In recent investigations, the most common metals have been used for alloying with Pt, including Ni, Cu, Ru, Mo and Sn [12]. Influence of the temperature on rate of the ethanol oxidation for Pt₃Sn/C, PtRu/C and Pt/C electrocatalysts is investigated [13]. The results display reducing temperature, and the oxidation of adsorbed carbon monoxide on PtRu increases. In another research, the effect of different atomic ratios of PtRuMo/C and PtRuFe/C on MOR activity is evaluated and compared to PtRu/C [14]. The outcomes exhibit that activity of Pt₅Ru₄Fe/C and Pt₄Ru₃Mo₃/C is higher by 98% and 260% than PtRu/C, respectively. Jeon et al. [15] studied on 63 atomic ratios of PtRuCu/C to find the most suitable electrocatalyst for MOR activity. The outcomes exhibit that the greatest MOR activity is related to Pt₆₆Ru₁₇Cu₁₇/C. Also, this catalyst in chronoamperometric and cyclic voltammetry tests has 86% and 26% higher activity than Pt₅₀Ru₅₀/C, respectively. Wang et al. [16] studied several atomic ratios of PtRuNi/C to determine the optimum atomic ratio for MOR. They found 6:3:1 atomic ratio is the most optimum composition. As well as, the peak current of this catalyst is gained with a value of 14.7 mA cm⁻². The ternary alloy of PtCoRu/C is introduced and studied for MOR [17]. The outcomes depict Pt₁₈Co₆₂Ru₂₀/C has the highest stability and activity, among the other electrocatalysts. The ternary Pt₄₅Ru₄₅Ni₁₀/C, Pt₄₅Ru₄₅Fe₁₀/C and Pt₄₅Ru₄₅Co₁₀/C alloys are synthesized and evaluated by electrochemical and physical tests [18]. Based on the gained outcomes, the greatest mass activity belongs to the Pt₄₅Ru₄₅Fe₁₀/C (2.6 A/g catal). Also, the largest specific activity is related to the Pt₄₅Ru₄₅Ni₁₀/C, with a value of 150 mA/m². Influence of the nanoparticles of platinum (1, 2 and 3 nm) on catalyst layers of a PEM fuel cell is studied [19].

According to the obtained results, the kinetics of the electrochemical reactions is improved considerably. In recent researches, other carbon supports such as graphene (Gr) and carbon nanotubes (CNTs), because of the good electronic properties, are utilized as the catalyst support [20]. For instance, 80 wt% PtRu/Gr is synthesized and used for MOR [21]. Based on the results, the activity of this catalyst is high, and Gr can be an appropriate supporting for high loading. The PtRu/CNT is fabricated by the two-step spontaneous deposition method for MOR in a solid polymer fuel cell (SPFC) [22]. According to the conducted evaluations, this type of catalyst can diminish the overall cost and increase the system efficiency. In order to increase the durability of catalyst, the Pt/carbon nano-fiber (CNF) catalysts with three different temperatures of 550, 650 and 700 °C are fabricated and analyzed [23]. The results indicate that Pt/CNF650 has the highest values of mass activity (23 A/mg-Pt) and electrochemically active surface area (ECSA) (32 m²/g Pt). The impacts of CNF materials as the support for PtRu nanoparticles for MOR applications are investigated [24]. Based on the TEM images, nanoparticles have a good distribution on the surface of support, as well as the values of ECSA are computed to be 110–140 m²/g Pt. The performance of PtRu and PtRuNi alloys on the support of MW-CNT for the MOR of fuel cell is evaluated [25]. The outcomes show that the optimal ratios for PtRuNi and PtRu are 8:1:1 and 8:2, respectively. The ternary formulation PtRuFe-supported N-doped graphene is synthesized and evaluated for MOR of the DMFC [26]. According to the obtained findings, the maximum power density is 112 mW/cm². In another research, the Pt-Ru-Fe ternary alloy on carbon support is synthesized for MOR application [27]. By using the electrochemical tests, the roles of Ru and Fe in the ternary catalyst are evaluated. According to the obtained findings, at the voltage of 0.45 V versus RHE, the MOR activity of Pt₃Ru₂Fe/C is 2.5 times higher than that of PtRu/C. A novel type of ternary Fe_{1-x}PtRu_x NCs is fabricated and introduced for MOR [28]. Based on the evaluations, Fe₃₅Pt₄₀Ru₂₅ catalyst has a suitable performance and activity.

The methanol oxidation activity of Pt₃Ru₂Fe/C was ca. 2.5 times higher than that of PtRu/C at 0.45 V versus RHE.

Yang et al. [29] introduced the PtAu/N-doped graphene (N-G) as catalyst for MOR. This catalyst with 3:1 atomic ratio of Pt/Au illustrates a suitable durability and activity for utilizing in fuel cell. In another investigation, Pt/CNT is used for MOR and ORR of a low-temperature fuel cell [30]. According to the outcomes of electrochemical and physical tests, because of the high specific surface of CNT, the activity increases and overpotential of MOR reduces. In a comprehensive evaluation, Pt/CNT with 12 wt% of platinum loading is synthesized for MOR and compared to the 29 wt% Pt loading of Pt/C [31]. The results indicate that by utilizing Pt/CNT, the power density increases by twice, and fuel cell voltage increases by 10%.

In this work, in order to improve the methanol oxidation reaction (MOR), five electrocatalysts including PtRu/C, PtRu₄Fe₅/SW-CNT, PtRu₄Fe₅/MW-CNT, PtRu₄Fe₅/Gr and PtRu₄Fe₅/C are synthesized and assessed. The performance and activity of synthesized electrocatalysts are evaluated by the physical and electrochemical measurements. Also, a micro-direct methanol fuel cell (μ -DMFC) is fabricated, in which the steps of fabrication are described. In continuation, according to the performed tests, the optimal electrocatalyst is selected and employed as anodic catalyst of the μ -DMFC. Finally, its performance is compared to the commercial Pt/C catalyst by the polarization curves.

2 Experimental section

In this section, the steps of fabrication of electrocatalysts and membrane electrode assembly (MEA) are proposed. Also, operation conditions of the physicochemical and electrochemical measurements are described.

2.1 MEA fabrication

2.1.1 Membrane purification procedure

In this investigation, Nafion 117 (with a thickness of 183 μm) was utilized as solid polymer electrolyte. First, Nafion was washed in a boiling 5% solution of hydrogen peroxide (H_2O_2), for 90 min at 80 $^\circ\text{C}$. In continuation, it was washed by boiling DI water for 90 min at 80 $^\circ\text{C}$. Then, the membrane was transferred to the 0.5 M sulfuric acid (H_2SO_4) for 90 min in order to convert into the acid form. At the end, to remove any impurities, the membrane was transferred to the boiling DI water for 90 min. The membrane was stored in DI water at room temperature before its usage in $\mu\text{-DMFC}$.

2.1.2 Synthesis of MOR nano-electrocatalysts

To synthesize the nano-alloys of Pt/Ru/Fe on Vulcan XC-72 carbon black, graphene (Gr) supports, multi-walled carbon nanotube (MW-CNT) and single-walled carbon nanotube (SW-CNT), the modified polyol method is used. Also, the CNTs used are commercial and were supplied from Plasma Chem. First, 50 mg of Vulcan XC-72 in 15 ml of ethylene glycol was sonicated for 20 min. The certain amounts of $\text{NH}_4\text{Fe}(\text{SO}_4)_2$, RuCl_3 and $\text{H}_2\text{PtCl}_6 \cdot 6\text{H}_2\text{O}$ were dissolved into the mixture obtained from the previous step. In continuation, 25 ml of ethylene glycol was added into the solution and sonicated for 20 min. The pH of solution was adjusted with 1 M NaOH. The resulting mixture was heated for 12 h until the nanoparticles of Pt, Ru, and Fe were formed on carbon supported. The final mixture was centrifuged to separate the solid particles. After washing several times with DI water, the final product was dried in an oven for 24 h at 80 $^\circ\text{C}$. The final powder catalysts have been named as PtRu/C, PtRu₄Fe₅/SW-CNT, PtRu₄Fe₅/MW-CNT, PtRu₄Fe₅/Gr and PtRu₄Fe₅/C. The loading of metals is adjusted to be wt 10%.

2.1.3 Preparation of electrodes

To fabricate the electrodes of anode and cathode, carbon paper is utilized as under layer. In order to clean the surface of carbon paper, it was washed by acetone for 20 min and dried in an oven at 80 $^\circ\text{C}$. In next step, the catalyst ink was prepared by dispersing the catalyst powder (2.5 mg) with a 500 μl of ethanol, followed by 20 μl of 5% wt Nafion solution. In order to get a uniform suspension, the mixture was sonicated for 1 h. Finally, the prepared catalyst ink was sprayed onto the surface of electrodes. The total loading of catalyst for anode and cathode sides is considered to be 3 and 2 mg cm^{-2} , respectively. Two electrodes were placed across the solid membrane (Nafion 117). The MEAs were fabricated utilizing a hot press that applied 150 kg/cm^2 of pressure at 130 $^\circ\text{C}$ for 2 min. The more information about this hot pressing method can be found in Ref. [12]. Finally, to evaluate the performance of fabricated MEA, it was employed in the $\mu\text{-DMFC}$. Figure 1 exhibits the illustrations of nano-electrocatalysts synthesized, MEA synthesized and fabricated $\mu\text{-DMFC}$ after the final montage.

2.2 Physicochemical characterizations

In this study, for evaluating the structural specifications, four physical measurements consisting of XRD, SEM, TEM and EDS have been considered. The mentioned tests investigate the

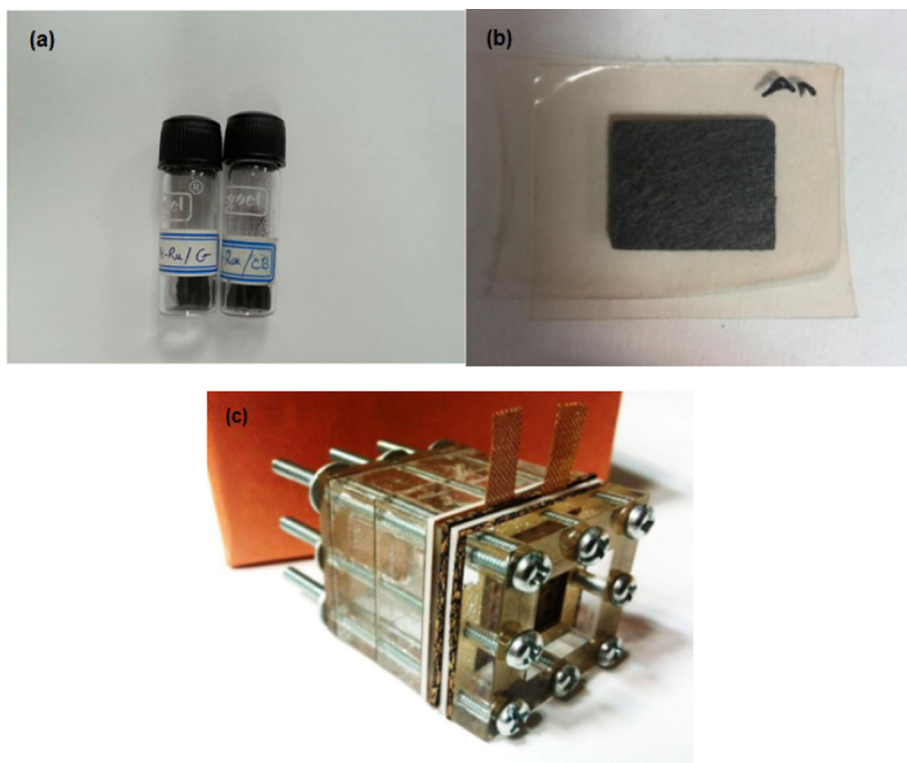


Fig. 1 The illustrations of nano-electrocatalysts synthesized (a), MEA synthesized (b), and fabricated μ -DMFC after final montage (c)

morphology, size of nanoparticles, distribution, and the atomic ratio of synthesized electrocatalysts. X-ray diffraction (XRD) was carried out for synthesized nano-electrocatalysts. This test was performed by XPERT MPD Philips, and using $\text{CuK}\alpha$ radiation at 40 kV, 30 mA and a scan rate of 15 min^{-1} . To evaluate morphology of the powder catalysts, the scanning electron microscopy (SEM) was performed with the magnification of 3000–30,000. This test was implemented by Philips XL30 operated at 20 kV. To confirm the distribution of the nanoparticles, the transmission electron microscopy (TEM) test was utilized. Moreover, in order to validate the atomic ratio of alloys and determine the binding energy, energy-dispersive X-ray spectroscopy (EDS; Model XL30, Philips Co.) was employed.

2.3 Electrochemical tests

The electrochemical tests have been carried out by beaker-type three-electrode cell. All electrochemical tests were performed in a mixture of 1 M CH_3OH and 0.5 M H_2SO_4 at 25°C . In order to eliminate the oxygen of solution, argon gas (Ar) was purged into the solution for 30 min. Platinum mesh is employed as counter electrode, an Ag/AgCl (saturated KCl-filled) is exploited as reference electrode, and glassy carbon (with a diameter of 2 mm) is utilized as working electrode. To assess the electrocatalytic activity of powder catalysts, the cyclic voltammetry (CV) measurement was employed [32]. The MOR activity was measured by the cyclic voltage between 0.2 and 1.1 V, at the scan rates of 150 and 50 mVs^{-1} . In

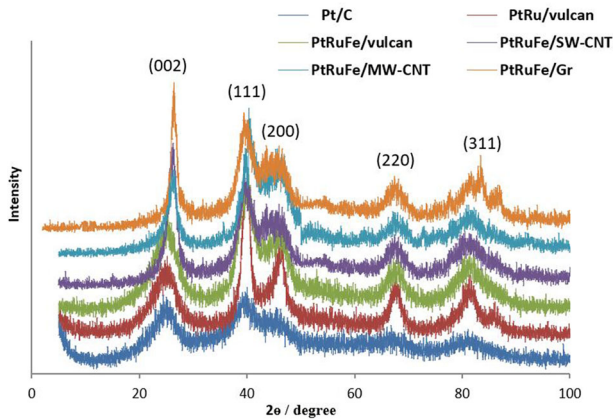


Fig. 2 The XRD patterns of synthesized nano-electrocatalysts

Table 1 A summary of structural properties for nano-electrocatalysts

Catalyst	(1 1 1) peak position (°)	Crystallite size (nm)	Specific surface area of catalyst (m ² /g (Pt))
Pt/C	39.5	3.7	75.8
PtRu/C	39.9	3.2	87.6
PtRuFe/C	39.84	2.7	103.8
PtRuFe/SW-CNT	39.65	5.4	51.9
PtRuFe/MW-CNT	39.72	8.8	31.9
PtRuFe/Gr	39.69	4.9	57.2

this investigation, to evaluate the catalytic performance of synthesized electrocatalysts, the electrochemical surface area (ESA) is computed by using the obtained results of CV tests. The high values of ECSA exhibit the reaction is desirable for electrochemical for MOR [33]. For each electrode, ESA can be computed as follows [34]:

$$\text{ESA} = \frac{Q_H}{([Pt] \times 0.21)} \quad (4)$$

In this formula, Q_H (mC/cm²) denotes the required charge for desorption and adsorption of hydrogen, $[Pt]$ (mg/cm²) denotes the loading of Pt on the electrode surface, and 0.21 belongs to the required charge for oxidizing the hydrogen. For calculating ECSA, the desorption is considered.

3 Results and discussion

In this section, the morphology and activity of synthesized nano-electrocatalysts are assessed. Hence, the results of physical and electrochemical tests are discussed, and the performance of MEA is assessed by polarization curves.

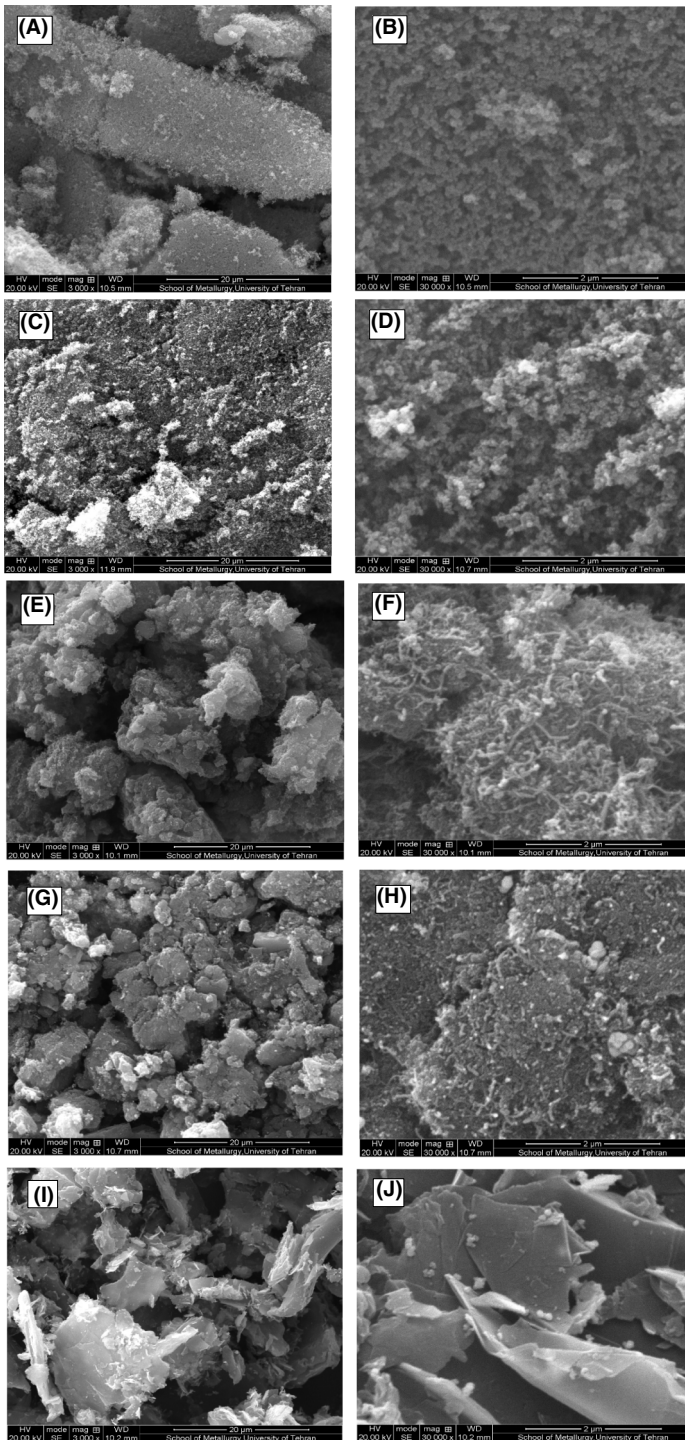


Fig. 3 SEM images of the synthesized electrocatalysts with a magnification of 3000 and 30,000: PtRu/C (a, b), PtRuFe/C (c, d), PtRuFe/SW-CNT (e, f), PtRuFe/MW-CNT (g, h), and PtRuFe/Gr (i, j)

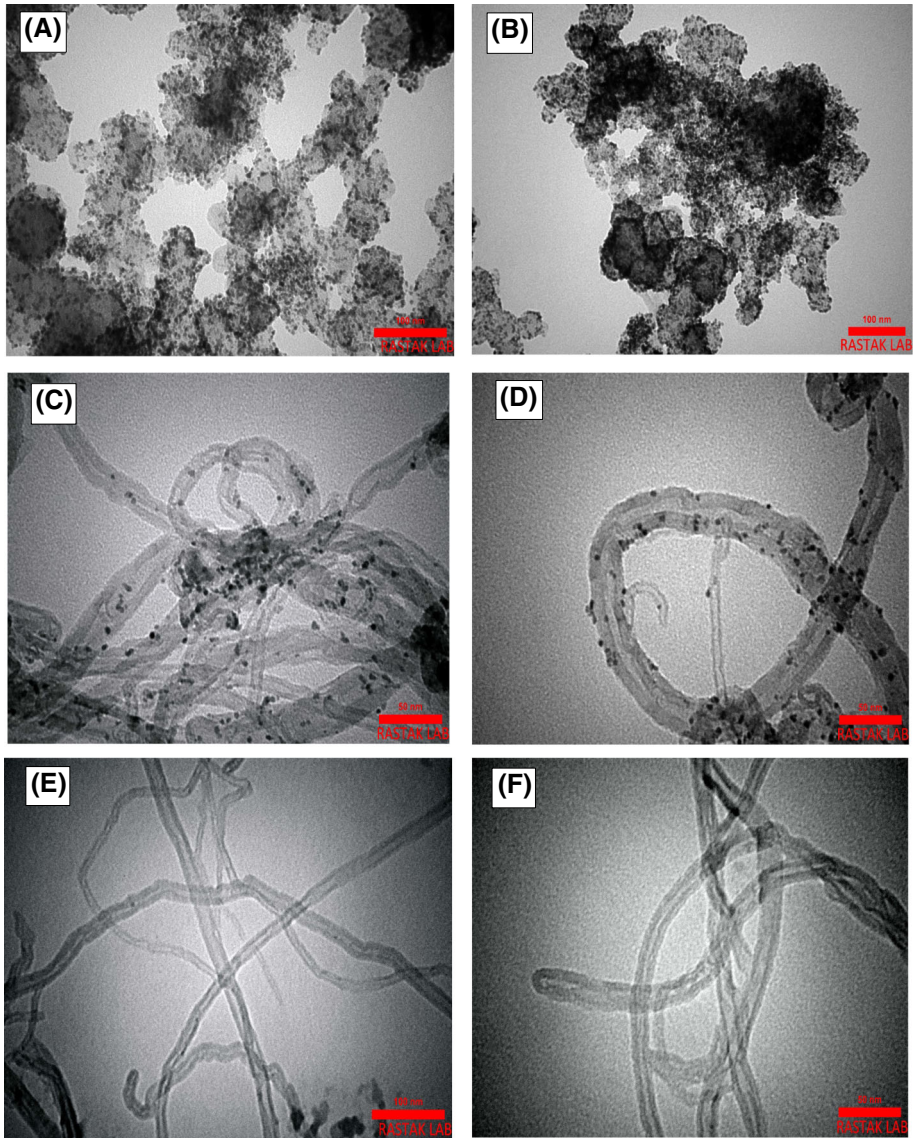


Fig. 4 TEM images of the synthesized electrocatalysts: PtRu/C (a, b); PtRuFe/SW-CNT (c, d); oxidized CNT (e, f)

3.1 Physicochemical measurements

Figure 2 exhibits the XRD patterns of synthesized electrocatalysts. The peak at $2\Theta = 39.5^\circ$ proves the Pt (111) on the carbon base. This peak indicates that particles of Pt were reduced on the supports successfully. Four peaks which are related to the Pt (1 1 1), (2 0 0), (2 2 0) and (3 1 1) can be seen in all of the electrocatalysts. The wide peak at $2\Theta = 26^\circ$ is associated with carbon sheets (0 0 2), which can be seen in all of the electrocatalysts. In all of the five electrocatalysts, the peak of Pt (1 1 1) was shifted to the higher 2Θ values (about 0.2° – 0.5°), which indicates the formation of an alloy between Pt and Ru and Fe. The outcomes of XRD

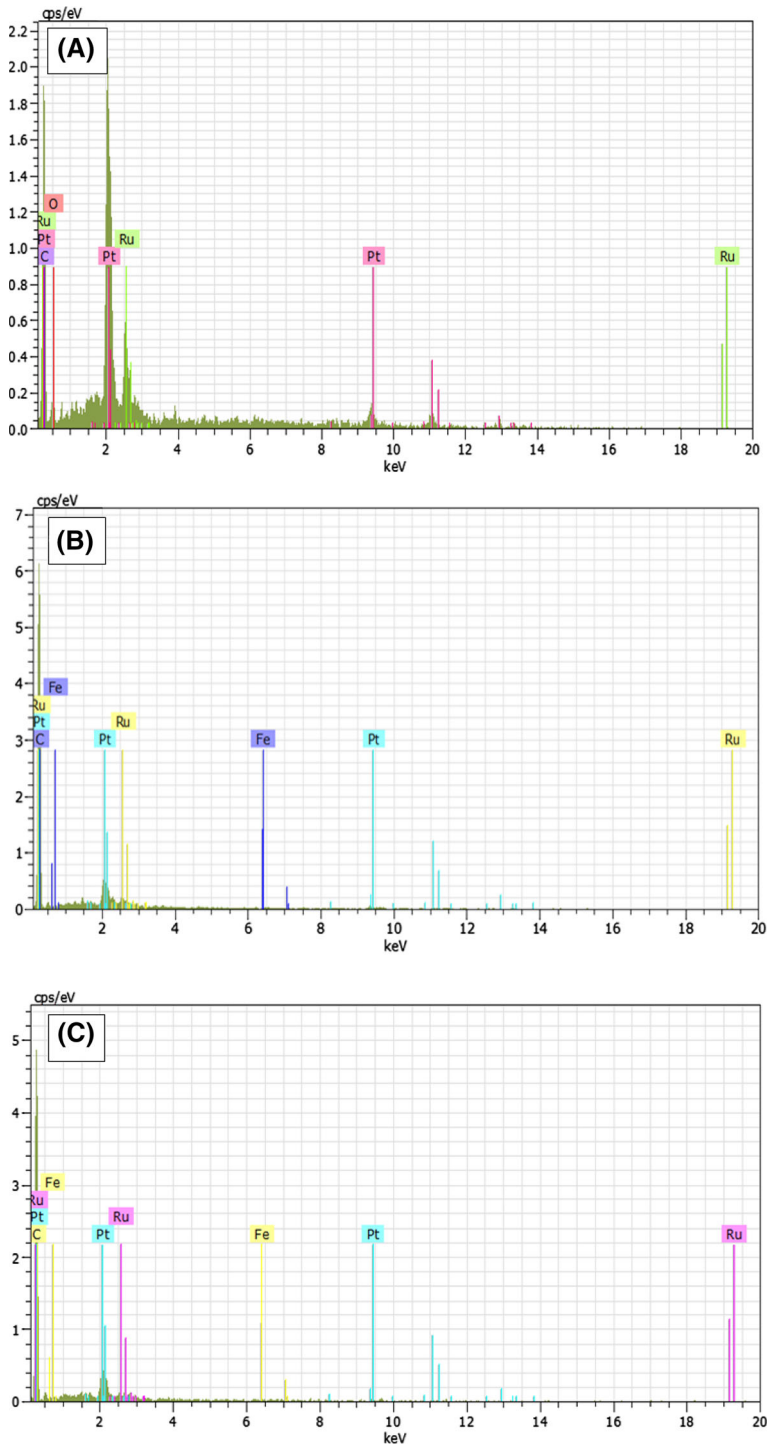


Fig. 5 The results of EDS test for synthesized nano-electrocatalysts: PtRu/C (a), PtRuFe/C (b), PtRuFe/SW-CNT (c), PtRuFe/MW-CNT (d), and PtRuFe/Gr (e)

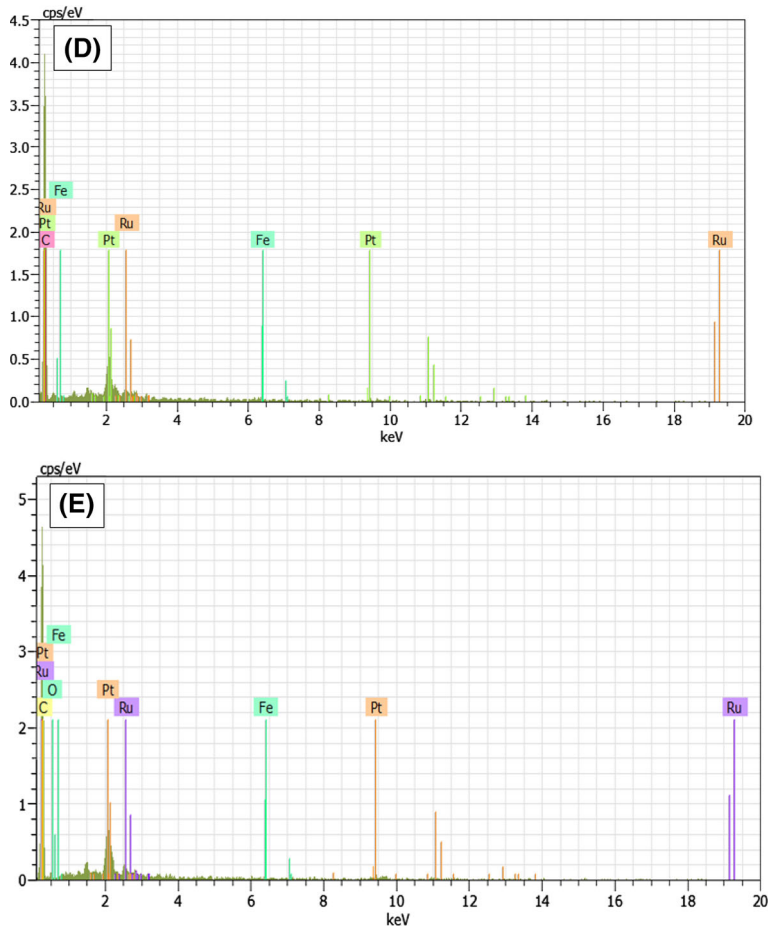


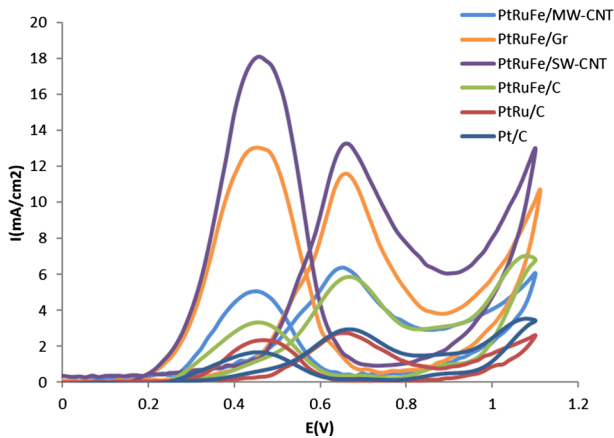
Fig. 5 continued

tests are summarized in Table 1. Figure 3 demonstrates the SEM images of synthesized electrocatalysts with a magnification of 3000 and 30,000. It can be noticed that the best nanoparticle dispersion occurred on graphene and carbon nanotubes supporting. Also, the Pt alloys were dispersed on carbon supports uniformly. Figure 4 illustrates the TEM images with the magnification of 50–100 nm. As can be observed, there exists a well-dispersed PtRu nanoparticle adlayer on the Vulcan. By comparing the TEM images for PtRuFe/SW-CNT (C and D) and PtRu/C, it can be confirmed that PtRuFe nanoparticles are distributed on the CNT walls quite uniformly and do not aggregate with each other to form larger clusters.

Figure 5 shows the results of EDS tests of nano-electrocatalysts. Based on the results, all metals have a peak in EDS figures, which indicates the process of synthesis has an acceptable accuracy. Table 2 presents the outcomes of EDS tests. It can be seen that obtained atomic ratios of EDS test are very near to the nominal atomic ratios. For instance, the nominal atomic ratio of PtRuFe/MW-CNT is considered to be 50:40:10, and the obtained atomic ratio by EDS measurement is gained by 52:39:9. These figures confirmed the alloying process has been done well.

Table 2 A summary of results of the EDS tests for nano-electrocatalysts

Catalyst	Nominal atomic ratio Pt:Ru:Fe	Obtained atomic ratios by EDS test Pt:Ru:Fe
PtRu/C	50:50:0	56:44:0
PtRuFe/C	50:40:10	52:37:11
PtRuFe/SW-CNT	50:40:10	53:40:7
PtRuFe/MW-CNT	50:40:10	52:39:9
PtRuFe/Gr	50:40:10	50:38:12

**Fig. 6** The results of CV tests for synthesized nano-electrocatalysts measured by potential cycling between 0.2 and 1.1 V. Scan rate = 150 mVs^{-1} , electrolyte: Argon purged 0.5 M H_2SO_4 + 1 M methanol solution**Table 3** The outcomes of the CV measurements for nano-electrocatalysts

Catalyst	Maximum current density ($\text{mA}\cdot\text{cm}^{-2}$)	Mass activity at the voltage of 0.5 V ($\text{A}/\text{mg Pt}$)
Pt/C	2.7	163
PtRu/C	3	188
PtRuFe/C	3.9	244
PtRuFe/SW-CNT	13.2	827
PtRuFe/Gr	11.6	727
PtRuFe/MW-CNT	4	251

3.2 Electrochemical measurements

Figure 6 illustrates the outcomes of CV tests of synthesized nano-electrocatalysts carried out for 50 cycles. The results of 50th cycle are presented in Fig. 6. All electrochemical tests were performed in a mixture of 1 M CH_3OH and 0.5 M H_2SO_4 at 25°C . It can be seen that among the synthesized nano-electrocatalysts, the largest value of maximum current density belongs to the PtRuFe/SW-CNT ($13.2 \text{ mA}/\text{cm}^2$), followed by PtRuFe/Gr ($11.6 \text{ mA}/\text{cm}^2$) and PtRuFe/MW-CNT ($4 \text{ mA}/\text{cm}^2$). Also, the least maximum current density is related to

Table 4 The results of ESA measurements for nano-electrocatalysts

Catalyst	The charge of hydrogen desorption (mC cm ⁻²)	Electrochemical active surface area (m ² /g (Pt))
Pt/C	19.2	57.2
PtRu/C	22.7	67.6
PtRuFe/C	25.4	75.5
PtRuFe/SW-CNT	71.3	212.2
PtRuFe/MW-CNT	38.2	113.7
PtRuFe/Gr	54.1	161

Table 5 The comparison of electrochemical tests results for this study with previous investigations

Parameter	This work (PtRu ₄ Fe ₅ /SW-CNT)	Lee et al. [14]	Jeon et al. [18]	Jang et al. [35]
Electrochemical active surface area (m ² /g catal)	212.2	Pt ₅ Ru ₄ Fe/C = 46.1 Pt ₄ Ru ₄ Fe ₂ /C = 31	Pt ₄₅ Ru ₄₅ Fe ₁₀ /C = 23 Pt ₄₅ Ru ₄₅ Co ₁₀ /C = 18	2D-GR/PtAu (PtAu 20%): GO 0.25 wt% = 41 GO 0.5 wt% = 50 3D-GR/PtAu (PtAu 20%): GO 0.25 wt% = 150 GO 0.5 wt% = 92
Mass activity in a voltage of 0.5 V (A/g catal)	827	Pt ₅ Ru ₄ Fe/C = 2.6 Pt ₄ Ru ₄ Fe ₂ /C = 1.14	Pt ₄₅ Ru ₄₅ Fe ₁₀ /C = 2.6 Pt ₄₅ Ru ₄₅ Co ₁₀ /C = 2.2	No reported

Table 6 The main specifications of synthesized MEAs for this investigation

Type of MEA	Pt loading for anode side (mg/cm ²)	Pt loading for cathode side (mg/cm ²)	Nafion loading for anode side (mg/cm ²)	Nafion loading for cathode side (mg/cm ²)
MEA (1): PtRuFe/SW-CNT (10% wt.)	3	2	1	1
MEA (2): Pt/C (10% wt.)	3	2	1	1

the commercial Pt/C (2.7 mA/cm²). Table 3 exhibits the results of CV measurements of synthesized electrocatalysts. PtRuFe/SW-CNT and Pt/C electrocatalysts have the highest and least mass activity, respectively. The results show that PtRuFe/SW-CNT has the most activity for oxidation of the methanol. Table 4 presents the obtained results of ESA for the commercial Pt-carbon black and synthesized nano-electrocatalysts. Among the synthesized electrocatalysts, the largest and lowest ESA belongs to the PtRuFe/SW-CNT (212.2 m²/g

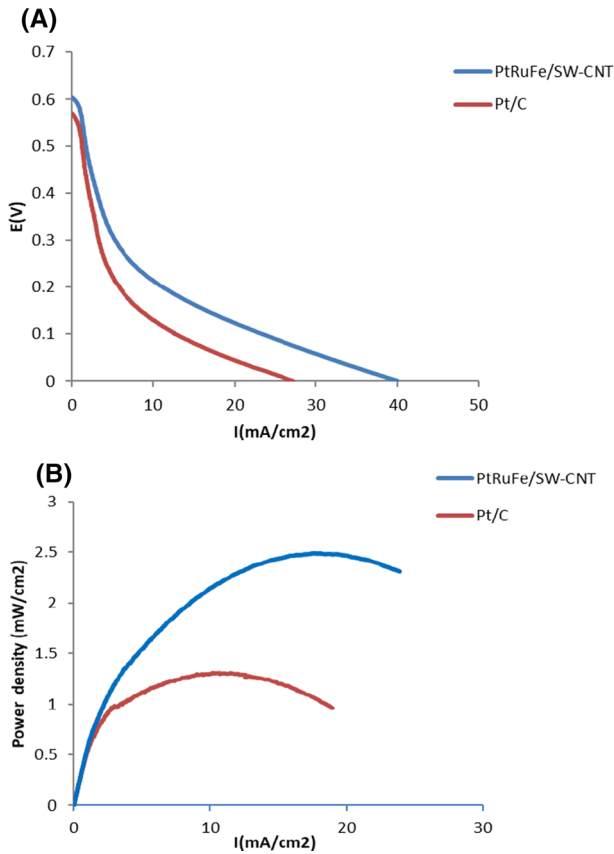


Fig. 7 The polarization (a) and power density–current density (b) curves of PtRuFe/SW-CNT and commercial Pt/C as anode catalyst, with 1 M methanol solution at room temperature

(Pt)) and Pt/C (57.2 m²/g (Pt)), respectively. Therefore, PtRuFe/SW-CNT catalyst is the most suitable candidate for employing in anodic catalyst of μ -DMFC. In continuation, the obtained results of electrochemical tests for PtRuFe/SW-CNT are compared to the previous investigations. Table 5 lists the comparison of the main parameters of this investigation with precious works. It can be seen that two parameters of mass activity and electrochemical surface area, which are very important to assess the performance of electrocatalysts, for this study are higher and better than previous works considerably.

3.3 Evaluation of MEA performance

According to the obtained results of physicochemical and electrochemical tests, the most optimum synthesized electrocatalyst is found to be PtRuFe/SW-CNT. So, this electrocatalyst is employed at the anode of μ -DMFC and compared to the Pt/C with polarization curves. For this purpose, two MEAs were synthesized (MEA (1) = PtRuFe/SW-CNT and MEA (2) = Pt/C). In these MEAs, all of the parameters are adjusted to be similar, except the kind of anode catalyst. Therefore, any difference in the performance of MEA depends on the activity of anodic catalyst. Table 6 represents the main specifications of synthesized

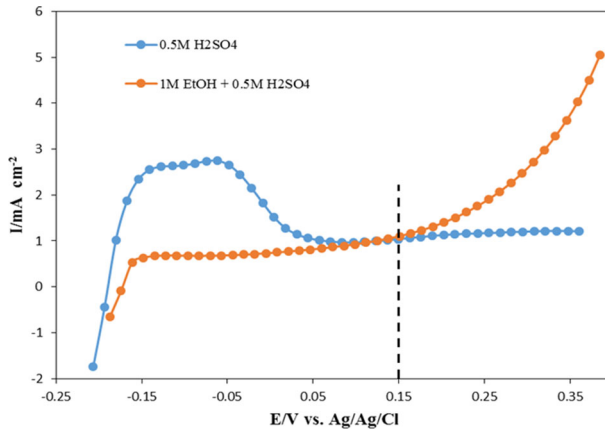


Fig. 8 The method of determining onset potential

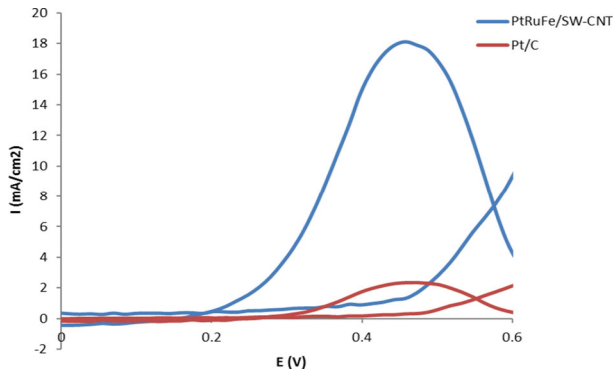


Fig. 9 The current density–onset potential diagram of MEA (1) and MEA (2)

MEAs. Figure 6 indicates the polarization and power density–current density curves for commercial Pt/C and PtRuFe/SW-CNT as the anode catalyst with 1 M methanol solution at room temperature (25 °C). According to this figure, the current density in zero voltage for MEA (1) and MEA (2) is obtained with the values of 40 mA/cm² and 27 mA/cm², respectively. In the same conditions, by employing PtRuFe/SW-CNT as the catalyst of anode, the current density increases by 48% compared to the commercial Pt/C. Also, the open-circuit voltage (OCV) for MEA (1) and MEA (2) is gained by 600 mV and 570 mV, respectively. It indicates the activity of PtRuFe/SW-CNT is higher than commercial Pt/C. Based on Fig. 7, the maximum power density for MEA (1) and MEA (2) is gained with the values of 2.5 mW/cm² and 1.3 mW/cm², respectively. An increase of 92.3% occurred in maximum power density, by utilizing PtRuFe/SW-CNT instead of Pt/C, as the catalyst of anode. One of the useful factors for evaluating the performance of electrocatalysts is onset potential of the MOR. Figure 8 shows the method of determining onset potential. Figure 9 demonstrates the current density–onset potential diagram of fabricated MEAs. Based on this figure, the onset potential of MEA (1) and MEA (2) is obtained by 0.23 V and 0.41 V, respectively. By alloying Pt with Ru and Fe, the activity of MOR is improved and electron production increases.

4 Conclusions

In this investigation, an effective anodic electrocatalyst for micro-direct methanol fuel cell is proposed. For this purpose, five nano-electrocatalysts consisting of PtRu/C, PtRu₄Fe₅/SW-CNT, PtRu₄Fe₅/MW-CNT, PtRu₄Fe₅/Gr and PtRu₄Fe₅/C are synthesized. The morphology and electrochemistry activity of the synthesized electrocatalysts are evaluated by the physical and electrochemical measurements, respectively. It was found PtRu₄Fe₅/SW-CNT is the optimal electrocatalyst and employed as the anodic catalyst of the μ -DMFC. Finally, its performance is compared to the Pt/C electrocatalyst, by polarization curves. The most remarkable outcomes of this research can be listed as follows:

- According to the XRD and SEM measurements, the formation and morphology of electrocatalysts are confirmed. Also, the size of nanoparticles is obtained in the range of 3–8 nm.
- Based on the EDS tests, the obtained atomic ratios are near to the nominal atomic ration, which displays the alloying process is carried out suitably.
- According to the TEM images, it can be confirmed that PtRuFe nanoparticles are distributed on the CNT walls quite uniformly and do not aggregate with each other to form larger clusters.
- Based on the CV measurements, the highest current density and mass activity belonged to the PtRu₄Fe₅/SW-CNT with the values of 13.2 mA/cm² and 827 A/g-Pt, respectively.
- The largest and lowest ESA belongs to the PtRuFe/SW-CNT (212.2 m²/g (Pt)) and Pt/C (57.2 m²/g (Pt)), respectively.
- By increasing the Ru atomic percentage, the alloying degree increases to 50%.
- By using PtRu₄Fe₅/SW-CNT at the anodic catalyst of μ -DMFC, the maximum power density and current density in zero-voltage increase by 92.3% and 48%, respectively. It shows the mass transfer of methanol is improved, and interaction between nanoparticles and SW-CNT support is proper.
- The onset potential of PtRu₄Fe₅/SW-CNT and commercial Pt/C is computed as 0.23 V and 0.41 V, respectively. It illustrates by alloying Pt with Ru and Fe, the activity of MOR is improved and electron generation increases.

The OCV of PtRu₄Fe₅/SW-CNT and commercial Pt/C is obtained as 600 mV and 570 mV, respectively. It demonstrates that the activation polarization of PtRu₄Fe₅/SW-CNT is lower than Pt/C.

References

1. M. Marefati, M. Mehrpooya, S.A. Mousavi, Introducing an integrated SOFC, linear Fresnel solar field, Stirling engine and steam turbine combined cooling, heating and power process. *Int. J. Hydrog Energy* **44**(57), 30256–30279 (2019)
2. M. Mehrpooya, B. Ghorbani, S.A. Mousavi, Integrated power generation cycle (Kalina cycle) with auxiliary heater and PCM energy storage. *Energy Convers. Manag.* **177**, 453–467 (2018)
3. B. Ghorbani, M. Mehrpooya, S.A. Mousavi, Hybrid molten carbonate fuel cell power plant and multiple-effect desalination system. *J Clean Prod* (2019)
4. A. Choudhury, H. Chandra, A. Arora, Application of solid oxide fuel cell technology for power generation—A review. *Renew. Sustain. Energy Rev.* **20**, 430–442 (2013)
5. M. Mehrpooya, M.M.M. Sharifzadeh, S.A. Mousavi, Evaluation of an optimal integrated design multi-fuel multi-product electrical power plant by energy and exergy analyses. *Energy* **169**, 61–78 (2019)
6. C.M. Branco et al., New approaches towards novel composite and multilayer membranes for intermediate temperature-polymer electrolyte fuel cells and direct methanol fuel cells. *J. Power Sour.* **316**, 139–159 (2016)

7. I. Kruusenberg et al., Highly active nitrogen-doped nanocarbon electrocatalysts for alkaline direct methanol fuel cell. *J. Power Sour.* **281**, 94–102 (2015)
8. L. Guo et al., Embedding Pt nanocrystals in N-doped porous carbon/carbon nanotubes toward highly stable electrocatalysts for the oxygen reduction reaction. *ACS Catal.* **5**(5), 2903–2909 (2015)
9. H. Liu et al., A review of anode catalysis in the direct methanol fuel cell. *J. Power Sour.* **155**(2), 95–110 (2006)
10. J. Wang et al., Highly active Pt-on-Au catalysts for methanol oxidation in alkaline media involving a synergistic interaction between Pt and Au. *Electrochim. Acta* **123**, 309–316 (2014)
11. P. Stonehart, Development of alloy electrocatalysts for phosphoric acid fuel cells (PAFC). *J. Appl. Electrochem.* **22**(11), 995–1001 (1992)
12. M.Z. Ghavidel, M.R. Rahman, E.B. Easton, Fuel cell-based breath alcohol sensors utilizing Pt-alloy electrocatalysts. *Sens. Actuators B Chem.* **273**, 574–584 (2018)
13. F. Colmati, E. Antolini, E.R. Gonzalez, Effect of temperature on the mechanism of ethanol oxidation on carbon supported Pt, PtRu and Pt₃Sn electrocatalysts. *J. Power Sour.* **157**(1), 98–103 (2006)
14. K.R. Lee, M.K. Jeon, S.I. Woo, Composition optimization of PtRuM/C (M = Fe and Mo) catalysts for methanol electro-oxidation via combinatorial method. *Appl. Catal. B* **91**(1–2), 428–433 (2009)
15. M.K. Jeon, J.S. Cooper, P.J. McGinn, Methanol electro-oxidation by a ternary Pt–Ru–Cu catalyst identified by a combinatorial approach. *J. Power Sour.* **185**(2), 913–916 (2008)
16. Z. Wang et al., *Novel Pt–Ru–Ni/C catalysts for methanol electro-oxidation in acid medium*. *Electrochem. Solid-State Lett.* **9**(1), A13–A15 (2006)
17. P. Strasser, Combinatorial optimization of ternary Pt alloy catalysts for the electrooxidation of methanol. *J. Comb. Chem.* **10**(2), 216–224 (2008)
18. M.K. Jeon et al., Pt₄₅Ru₄₅M₁₀/C (M = Fe Co, and Ni) catalysts for methanol electro-oxidation. *Catal. Today* **132**(1–4), 123–126 (2008)
19. C. Cheng et al., Effect of Pt nano-particle size on the microstructure of PEM fuel cell catalyst layers: Insights from molecular dynamics simulations. *Electrochim. Acta* **55**(5), 1588–1597 (2010)
20. Z. Guo et al., Carbon nanotube-supported Pt-based bimetallic catalysts prepared by a microwave-assisted polyol reduction method and their catalytic applications in the selective hydrogenation. *J. Catal.* **276**(2), 314–326 (2010)
21. S. Bong et al., Graphene supported electrocatalysts for methanol oxidation. *Electrochem. Commun.* **12**(1), 129–131 (2010)
22. W.-C. Chang, M.T. Nguyen, Investigations of a platinum–ruthenium/carbon nanotube catalyst formed by a two-step spontaneous deposition method. *J. Power Sour.* **196**(14), 5811–5816 (2011)
23. D. Sebastián et al., Enhanced oxygen reduction activity and durability of Pt catalysts supported on carbon nanofibers. *Appl. Catal. B* **115**, 269–275 (2012)
24. D. Sebastián et al., The effect of carbon nanofiber properties as support for PtRu nanoparticles on the electrooxidation of alcohols. *Appl. Catal. B* **132**, 13–21 (2013)
25. Y. Zhao et al., Electrodeposition of Pt–Ru and Pt–Ru–Ni nanoclusters on multi-walled carbon nanotubes for direct methanol fuel cell. *Int. J. Hydrog. Energy* **39**(9), 4544–4557 (2014)
26. M. Rethinasabapathy et al., Ternary PtRuFe nanoparticles supported N-doped graphene as an efficient bifunctional catalyst for methanol oxidation and oxygen reduction reactions. *Int. J. Hydrog. Energy* **42**(52), 30738–30749 (2017)
27. T. Kim et al., Electronic modification effects induced by Fe in Pt–Ru–Fe ternary catalyst on the electrooxidation of CO/H₂ and methanol. *J. Oleo Sci.* **61**(3), 127–134 (2012)
28. D.-Y. Wang et al., Simple replacement reaction for the preparation of ternary Fe_{1-x}PtRu_x nanocrystals with superior catalytic activity in methanol oxidation reaction. *J. Am. Chem. Soc.* **134**(24), 10011–10020 (2012)
29. G. Yang et al., Pt–Au/nitrogen-doped graphene nanocomposites for enhanced electrochemical activities. *J. Mater. Chem. A* **1**(5), 1754–1762 (2013)
30. Y. Lin et al., Platinum/carbon nanotube nanocomposite synthesized in supercritical fluid as electrocatalysts for low-temperature fuel cells. *J. Phys. Chem. B* **109**(30), 14410–14415 (2005)
31. H. Tang et al., High dispersion and electrocatalytic properties of platinum on well-aligned carbon nanotube arrays. *Carbon* **42**(1), 191–197 (2004)
32. A. Farzaneh et al., 3-D mesoporous nitrogen-doped reduced graphene oxide as an efficient metal-free electrocatalyst for oxygen reduction reaction in alkaline fuel cells: role of π and lone pair electrons. *Electrochim. Acta* **222**, 608–618 (2016)
33. Y. Xu et al., Ultrasonication-switched formation of dice-and cubic-shaped fullerene crystals and their applications as catalyst supports for methanol oxidation. *Mater. Horizons* **1**(4), 411–418 (2014)

34. B. Wu et al., High dispersion of platinum–ruthenium nanoparticles on the 3, 4, 9, 10-perylene tetracarboxylic acid-functionalized carbon nanotubes for methanol electro-oxidation. *Chem. Commun.* **47**(18), 5253–5255 (2011)
35. H.D. Jang et al., Three-dimensional crumpled graphene-based platinum–gold alloy nanoparticle composites as superior electrocatalysts for direct methanol fuel cells. *Carbon* **93**, 869–877 (2015)